

1N-02-CR  
62366  
p- 42

**Experimental Study  
of a  
Vortex Subjected to Imposed Strain**

**Final Report  
NASA Grant NAG 2-389  
Aug 1991**

**Ronald L. Panton  
Professor, Principal Investigator  
and  
Kirk E. Stifle  
Graduate Student**

**Department of Mechanical Engineering  
University of Texas, Austin, TX 78712**

(NASA-CO-152757) EXPERIMENTAL STUDY OF A  
VORTEX SUBJECTED TO IMPOSED STRAIN Final  
Report (Texas Univ.) 42 p

CSCL 61A

APR-1992

Unclas  
00/02 0002166

## EXPERIMENTS ON TRAVELING VORTEX BREAKDOWN WAVES

Kirk E. Stifle\* and Ronald L. Panton\*\*

Department of Mechanical Engineering  
University of Texas, Austin, TX 78712

### ABSTRACT

An experimental project was undertaken to investigate the character of vortex breakdown with particular regard to the wave-guide theories of vortex breakdown. A rectangular wing based on the NACA 0012 airfoil was used to produce a trailing vortex which convected downstream without undergoing breakdown. Dye marked the vortex location. A disturbance was then introduced onto the vortex using a small moving wire to 'cut' the vortex. The development of upstream and downstream propagating disturbance waves was observed and the propagation velocities measured. The downstream traveling wave produced a structure similar in appearance to a vortex breakdown. The upstream traveling wave produced a moving, swirling, turbulent region that was not a vortex breakdown. The waves moving in either direction have the same swirl velocity profiles but quite different axial velocity profiles. The upstream disturbance (turbulence) moved into a flow with an axial velocity profile that had a wake-like defect in the core region. The downstream moving vortex breakdown moved into a flow with a jet-like overshoot in the core region. The fact that no breakdown was observed for the wake-like defect and breakdown was observed for the jet-like overshoot is not consistent with CFD calculations. Although there are not a lot of examples, CFD results show breakdown for both types of profiles. The longitudinal and swirl velocity profiles were documented by LDV measurement. Wave velocities, swirl angles, and swirl parameters are reported.

---

\* Graduate research assistant

\*\* Professor, Associate Fellow AIAA

## NOMENCLATURE

$K$	constant proportional to circulation
$L$	length, cm
$R$	nondimensional radius, $r/r^*$
$Re$	Reynolds number, $Wr^*/\nu$
$Ro$	Rossby number, $W/r^*\Omega$
$T$	arrival time of disturbances
$T_0$	freestream convection time, $c/U_0$
$U(r)$	dimensional axial velocity, cm/s
$U(R)$	nondimensional axial velocity
$U_0$	freestream velocity
$U_1$	amount of axial defect (or excess)
$U_w$	nondimensional wave velocity, $U_{wave}/U_0$
$U_{wave}$	absolute wave velocity, cm/s
$V(r)$	dimensional tangential velocity, cm/s
$V(R)$	nondimensional tangential velocity
$W$	axial velocity at the location of maximum swirl, cm/s
$Z(R)$	nondimensional relative wave velocity
$c$	centerline chord length, cm
dwn	downstream disturbance
$q$	swirl parameter, determined from curve fits
$r$	radial coordinate
$r^*$	core radius, location of maximum tangential velocity
$x$	axial coordinate
up	upstream disturbance

$\alpha$	angle of attack
$\delta$	velocity defect or excess
$\phi$	swirl angle, $\tan^{-1}(V(R)/U(R))$
$\Omega$	limit of $(V/r)$ as $r$ approaches zero, $\lim_{r \rightarrow 0} (V/r) = aK/2v$

subscripts

axial	axial
tang	tangential
vmax	location of maximum tangential velocity

## INTRODUCTION

The term 'vortex breakdown' is used to describe the sudden and often drastic change in structure that occurs in vortex flows. Commonly cited characteristics of vortex breakdown include a stagnation point on the axis and a region of flow reversal. (However, Bradshaw<sup>1</sup> suggests that complete stagnation is not a necessary part of vortex breakdown in a turbulent vortex).

Strong vortices are generated by conventional wing-tips, flap ends, strakes (leading edge extensions), and delta wings. Because these vortices persist for long periods of time, they present a hazard to other aircraft, particularly at airports while landing. Because new aircraft (particularly military) are being designed to maneuver at high angles of attack, the question of vortex breakdown has become increasingly important. During high angle of attack maneuvering, the breakdown may move onto the wing. This is particularly true for wings with high sweep angles such as delta wings. This changes the pressure distribution on the wing and greatly effects the pitching moment.<sup>2</sup> The breakdown position is not stationary but may oscillate randomly. This can cause aft control surfaces and structure to vibrate.

There are several theories or models of the physics of vortex breakdown. The purpose of this research is to experimentally investigate the growth and propagation of large perturbations on a

vortex. The results are interpreted in terms relevant vortex breakdown theories and vortex breakdown criteria.

## BACKGROUND

Recent reviews by Escudier<sup>2</sup>, Leibovich<sup>3</sup>, and Stuart<sup>4</sup> show that interest in vortex breakdown is strong. These reviews support the idea that breakdown is a transition between a supercritical upstream flow and a subcritical downstream flow. Even so, they note that general agreement on a theory which adequately describes vortex breakdown has not yet been achieved. Hall<sup>5</sup> and recently, Escudier<sup>2</sup> classify the theories of vortex breakdown into categories based on 1) instability of the upstream flow, 2) stagnation of the core flow or external pressure gradient, and 3) wave phenomena on the vortex core.

The first viewpoint is that vortex breakdown is a result of hydrodynamic instability. The upstream flow is unstable to axial or spiral disturbances which grow until a critical amplitude is reached. At this point, the flow transitions to a new type of stable flow pattern, much like the transition to turbulence. This view was put forth in early research on vortex breakdown<sup>6</sup> but it is not supported by recent experimental evidence.<sup>4</sup> Since the flow observed upstream of the breakdown is theoretically stable,<sup>3,4</sup> the instability theory is no longer thought to be a primary cause of vortex breakdown. Ironically, the downstream flow is frequently unstable and does ultimately become turbulent. This has raised new questions regarding the role instability plays in vortex breakdown.<sup>7,8</sup>

The second view is that vortex breakdown occurs as result of stagnation on the vortex centerline. Vortex breakdown is thought to be analogous to separation in a boundary layer. This suggests that an external pressure gradient initiates the process of vortex breakdown. In other words, the existence of a small external pressure gradient seems to be a necessary part of this viewpoint. This view is supported by Hall's<sup>5</sup> analysis that a small pressure gradient in the external flow is significantly amplified at the vortex core. If the stagnation view is correct, then in the

absence of any external pressure field, an initial disturbance would not develop into a vortex breakdown.

The last view is that vortex breakdown is a result of nonlinear wave propagation.<sup>3</sup> The vortex is thought of as a wave-guide in which upstream propagating waves are trapped and amplified. The wave speed depends on the strength or amplitude of the wave, and hence on the strength of the disturbance mechanism. The waves collect at a location where the wave velocity equals the oncoming stream velocity. At this location, the waves can no longer propagate upstream and a steady breakdown occurs.<sup>3</sup> This view is analogous to a hydraulic jump or a shock wave seeking a stationary position in a flow.

An element of all the above views is the idea of conjugate flow states. This is the existence of two swirling flows where the fluid particles have the same angular momentum and total head but the vortex has a different core size. The idea being that vortex breakdown is a transition between a supercritical upstream flow and a subcritical downstream flow. This view, originally proposed by Benjamin<sup>9</sup>, is continued by others, with the most recent being Spall and Gatski<sup>10</sup>, and Stuart.<sup>4</sup>

Only a few experiments related to waves on vortices have been performed. Maxworthy, *et. al.*<sup>11</sup> induced waves on a vortex in a rotating tank. They observed six types of waves which propagated along the vortex core: 1) helix, 2) standing wave, 3) kink wave, 4) kink plus trailing disturbance, 5) disturbance with increasing wavelength, and 6) axisymmetric. The axisymmetric wave was the only wave which disrupted the vortex. The axisymmetric wave was not a breakdown but did lead to vortex breakdown.

Reynolds and Abtahi<sup>12</sup> experimented on the leading edge vortex developing on a delta wing. Introducing disturbances into the core they observed a bulge which propagated downstream in the vortex core with a velocity much less than the fluid velocity in the core. They did not call this disturbance a breakdown. They were able to relate the wave speed to the wave amplitude for

'small amplitude' waves. In these experiments, the vortex velocity profiles are changing at different chord positions.

Stifle and Panton<sup>13</sup> and Stifle<sup>14</sup> subjected a trailing vortex from a straight flat -plate wing with a barb-like delta tip to large amplitude disturbances. They observed a downstream bulge very similar to a vortex breakdown. Nothing resembling vortex breakdown was observed to propagate upstream. The downstream breakdown propagated into an axial velocity which had a jet-like profile while the upstream disturbance propagated into a wake-like axial profile. Some unexplained inconsistencies in the quantitative data from these experiments led to abandoning this model for the present square-tipped NACA 0012 wing.

There have been many numerical investigations of vortex breakdown starting with Bossel<sup>15</sup> who used boundary layer equations. Investigations solving the full axisymmetric Navier-Stokes equations have also been undertaken, for example by Grabowski and Berger.<sup>16</sup> Recently, nonaxisymmetric calculations have been accomplished.<sup>17</sup> All these investigations have emphasized laminar vortex flows. The axial (frequently taken as uniform) and tangential velocity profiles are varied to study their effects on breakdown. Care should be taken when interpreting numerical results. Almost any combination of velocity profile will produce some type of breakdown. This breakdown will move to the front of the computational grid where it is stabilized by the initial conditions. Thus breakdown is a result of the computational grid and the initial conditions. This point has been discussed by Leibovich.<sup>18</sup>

The purpose of the present experimental research is to investigate the character of vortex breakdown with particular regard to the wave guide theories. In the experiments, a trailing vortex was produced which convected downstream without undergoing breakdown. The longitudinal and swirl velocity profiles were documented by LDV measurements. Disturbances were then introduced into the vortex using a moving wire to cut the vortex: a method similar to Maxworthy,

*et. al.*<sup>11</sup> and to Reynolds and Abtahi.<sup>12</sup> The development of upstream and downstream propagating waves was observed, their characteristics noted, and wave velocities measured.

## EXPERIMENTAL SETUP

A detailed description of the experimental apparatus is given by Stifle.<sup>14</sup> A horizontal water channel with a cross section 76.2 cm wide and 50.8 cm deep and 244 cm long (2.5 ft x 1.6 ft x 8 ft) was used for this experiment. A detailed description of the channel is given in Daigle.<sup>19</sup> In the present experiments, the channel was modified in one way. A one inch thick piece of plastic honeycomb was added to the inlet of the test section. This was done to destroy fluctuations from the upstream stilling tank that were disrupting the vortex motion.

The wing used in these experiments has been described previously.<sup>19,14</sup> It was machined from 6061-T6 aluminum on a numerical milling machine to a planform based on the NACA 0012 airfoil. The wing protruded through the free surface and was coupled to the output shaft of a reducing gear that was used to control the angle of attack. The rectangular wing had a chord length of 7.62 cm (3 in) and a span of 20.32 cm (8 in).

The wing produced a vortex that would convect through the 244 cm (8 ft) long test section and into the downstream stilling tank. As the angle of attack was increased, a helical disruption would appear downstream ( $x/c > 5$ ) on the vortex. This disruption was not a vortex breakdown. There was no region of flow reversal and no axial stagnation point. As the angle of attack was increased, the disruption would move upstream closer to the wing trailing edge. The angle of attack was kept below this level so that no disruptions occurred on the vortex while it was in the test section.

Black drafting ink, used as dye, was gravity feed into the vortex core with a stopcock controlling the dye flow rate. The dye was feed into the vortex through a 17.8 cm (7 in) long, 0.32 cm (0.125 in) slot milled into the underside of the wing. The slot was covered with an acrylic window so that dye could exit only at the edge of the airfoil. Flood lights were used to illuminate



the dye against a white background. The channel setup is shown in figure 1. Both high speed videos and still photographs were used for analysis purposes.

The flow velocity was varied from 11.6 cm/s to 25.7 cm/s. This gave a chord Reynolds number between  $0.7643 \times 10^4$  and  $1.69 \times 10^4$ . Although this is low from a flight standpoint, the vortex and its breakdown characteristics are not very sensitive to Reynolds number.<sup>20</sup> As a comparison, Reynolds and Abathi<sup>12</sup> had a Reynolds number between  $1.0 \times 10^4$  and  $6.2 \times 10^4$ .

Disturbances on the vortex core were introduced using cylindrical rods ranging in size from 0.107 cm (0.042 in) to 0.3175 cm (0.125 in) in diameter. These rods were used to cut the vortex by sweeping the rod through the vortex core in a motion perpendicular to the vortex axis. A spring mechanism was used to control the cut speed.

To avoid the flow adjustment region at the wing trailing edge the disturbances were introduced at a position approximately two chord lengths downstream. When perturbed, the vortex would break into two separate disturbances, an upstream disturbance and a downstream disturbance. A grid marked in one chord steps was filmed in the channel at the location where the vortex would be. From this data, a template was made to place over the high speed video monitor. The disturbances could then be tracked in one chord increments.

Quantitative measurements of the undisturbed vortex were taken with a TSI 9100-10, 3-component, 2 color LDV system used in backscatter mode. Only the longitudinal and swirl components of velocity were measured. Data were acquired using a Hewlett-Packard 1000 microcomputer with TSI and in-house software. The measurements were used to construct velocity profiles at axial locations of five, seven, ten, and fifteen chords downstream of the wing trailing edge. Profiles of the vortex were measured by moving the probe volume horizontally through the vortex. A staggered grid was used to cluster more points in the vortex core. The probe volume was moved in 2 mm (near vortex centerline) and 5 mm (away from centerline) steps.

A minimum of 500 data points were taken at each location and averaged to obtain mean velocity profiles.

## RESULTS

### Vortex Velocity Profiles

Figures 2 and 3 show typical axial and tangential velocity profiles from LDV measurements at the four downstream positions. The axial defect is roughly 35 percent and the swirl velocity varies from 40 to 60 percent of freestream depending on the axial location. The axial profiles were similar at all four locations while the tangential profiles showed a slight decrease in vortex strength with increasing downstream distance. The profiles are of the vortex produced at an angle of attack of  $12.14^\circ$  and freestream velocity of 22.6 cm/s. The profiles are similar to previous results.<sup>21,22</sup>

In order to quantify the data, the vortex profiles were fitted to the Q-vortex model.<sup>3</sup> The nondimensional velocity profiles are given by

$$V(R) = (q |\delta|/R) (1 - \exp(-R^2))$$

$$U(R) = 1 + \delta \exp(-R^2)$$

where

$$V(R) = V_{\text{tang}}/U_o$$

$$U(R) = U_{\text{axial}}/U_o$$

$$R = r/r^*$$

and

$$r^* = 1.12 (2\nu/a)^{1/2}$$

where  $\nu$  is the kinematic viscosity and  $a$  is an adjustable constant which depends on the core size.

The core radius,  $r^*$ , is the location where  $V(R)$  is maximum. The parameter  $q$ , called the swirl parameter by Lessen, *et. al.*<sup>23</sup>, is a measure of the maximum tangential velocity to the axial velocity excess or defect ( $U_o - U_{\text{axial}}(0)$ ). The parameter  $\delta$  is a measure of the ratio of the maximum axial velocity defect (or excess) to the freestream velocity. Figures 4 and 5 show a comparison of the

measured profiles with the curve fits. We were able to fit the axial velocity profiles very well. The tangential curve fit was able to capture the important results of the data such as the maximum swirl velocity, but the curve fit does not follow the data as well outside of the core region.

It is important to note that a wave traveling downstream with a speed greater than  $U_0$  sees a vortex with a jet-like axial velocity profile. Conversely, a disturbance traveling upstream against the flow sees a vortex with a defect or wake-like axial velocity profile. Figure 6 illustrates this.

### Visual Characteristics of Disturbances

When cut with a rod, the vortex would separate into two distinct disturbances with a clear space containing no dye between them. The downstream section would quickly develop into an axisymmetric bulge. The upstream section would form a kink which was quickly washed out by the oncoming fluid and was followed by the development of a turbulent, helical flow pattern. Figure 7 shows a general sketch of the events. The upstream disturbance propagates upstream at less than the freestream velocity and this entire group of events is carried downstream.

In all experiments, the downstream waves appeared as an axisymmetric bulge similar to a bubble type of vortex breakdown. Typical downstream breakdown waves are shown in figs. 8 and 9 (flow and propagation are from right to left). The breakdown bulge would move downstream with a velocity greater than the freestream velocity. The wave would retain its shape as it moved downstream. The breakdown bulge is similar to the type of disturbance Granger<sup>24</sup> produced in his experiments on vortex cores in pump inlets. The appearance of the downstream disturbances as breakdown bulges can be attributed to the formation of an axisymmetric type of wave. This wave is created by "cutting off" or momentarily stopping the axial core flow.<sup>11</sup>

The vortex downstream of the bulge breakdown did not exhibit any signs of disruption. There was only a slight spreading of the vortex core just downstream of the bulge. Fluid appeared to be drawn into the center of the disturbance from the rear, almost as if an object were being pushed into the bulge. This bulge breakdown has a very distinct wake behind it. Most bubble

type breakdowns on wing tip or delta wing vortices have more of a transition or turbulent region than a distinctive wake shape.<sup>20,25</sup>

We feel fairly confident that the downstream disturbances are vortex breakdowns. Faler and Lebiovich<sup>26</sup>, Escudier, *et. al.*<sup>27</sup>, Escudier and Zehnder<sup>28</sup>, and Maxworthy, *et. al.*<sup>11</sup> have reported vortex breakdowns similar to those observed in this experiment. The breakdowns in the above mentioned papers always propagated into a flow with an axial jet profile. As was mentioned in the previous section, the breakdowns observed in this experiment also propagate into an axial jet.

The upstream disturbance did not assume a steady shape but appeared as a swirling, helical flow pattern. Figures 10 and 11 show the typical appearance of the upstream disturbance. Even though the disturbance did have some structure, it was not a vortex breakdown. The disturbance did not show the kinking typical of a spiral type of breakdown.<sup>20</sup> There was no flow reversal and although a stagnation point was present when the vortex was initially cut, it would be washed downstream. This stagnation point would become indistinguishable within approximately one chord of the cut location.

There is a slight possibility that the upstream disturbance is a double helix type of vortex breakdown.<sup>6</sup> However, a helical type of breakdown is quite special and has never been observed on a wing tip or delta-wing vortex. Furthermore, the vortex shows a gradual increase in core size and not a sudden jump in core size characteristic of vortex breakdown.

### Wave Speeds

The disturbances were tracked as they moved downstream by placing a template over the video monitor as the video recordings were played back. Figure 12 is a typical space-time plot of the raw disturbance data. The times were normalized using  $c/U_0$ . The scatter from the upstream disturbance is roughly equal to or less than 20 percent while the downstream data have very little scatter. The upstream disturbance was difficult to track as it moved downstream because there was

not a sudden transition between the vortex and the disturbance. This causes much of the scatter in the upstream disturbance data.

Because the downstream propagating breakdown has a regular structure and a reasonably constant velocity we are comfortable calling it a wave. On the other hand, the upstream propagating disturbance does not have a well defined structure and one could easily argue that it is not a wave.

Figure 13 is a typical space-time graph of the ensemble averaged data. Both the upstream disturbance and downstream wave data tended to fall on a straight line. The data was curve fit with a straight line and the inverse slope of this line was used as the average velocity of the disturbance. All of the data points were used in the curve fit since the measurements were taken approximately three chords downstream of the cut location. This gives sufficient time for any transients to die out. Listed in Table 1 is the average downstream wave velocity.

As has been stated, wave theories of breakdown predict an increase in wave velocity with increasing vortex strength. There are a number of ways the strength of a vortex can be increased. Two ways used in this experiment were to increase the angle of attack and to increase the freestream velocity. Figure 14 shows the average disturbance velocities versus the angle of attack. There was a slight increase in the downstream wave velocity as the angle of attack was increased while the upstream disturbance velocity showed a decrease. Figure 15 is a graph of the average disturbance velocity versus freestream velocity. The downstream wave velocity would increase as the freestream velocity was increased and the upstream disturbance velocity decreased. The downstream wave velocity showed a decrease with decreasing probe size while the upstream disturbance velocity increased. Figure 16 shows this trend. This trend is similar to what Reynolds and Abtahi<sup>12</sup> observed.

Care must be taken when interpreting figures 14 and 16. The data for these graphs is very sparse and limited. These results are very preliminary and the increase (or decrease) in disturbance velocity is very small compared to the increase in the angle of attack or probe size.

### **Effect of Probe Size**

The initiation of the disturbance depended on the size of the probe and the speed at which the vortex was cut. As smaller probes were used, a faster cutting speed was needed to obtain a complete separation of the vortex into two sections. If there was no separation, no downstream bulge was observed. The smaller probe (0.107 cm) could be passed slowly through the vortex without any noticeable effect. If a more violent cutting motion was used, the vortex would disrupt into a structure similar to those obtained for the larger probes. No relationship between probe size and disturbance velocity was determined. This is different than results reported by Reynolds and Abtahi.<sup>12</sup> They found a linear relationship between wave amplitude and wave speed for small amplitude waves. Large amplitude waves diverged from this relationship. Our waves may have been large based on their definition. This may explain the difference.

The downstream wave always appeared as a bulge except at low speeds ( $U_o < 8$  cm/s). At low freestream velocities, the large probe (0.3175 cm) would create a very large disturbance that would completely obliterate the vortex. This probe created too large of a disturbance. The small probe (0.107 cm) would still create an axisymmetric wave. At higher freestream velocities, the small probe created a slightly smaller bulge than the large probe but there was no other significant visual difference between the waves.

### **Swirl Angles and Swirl Parameters**

From the fitted velocity profiles and the "wave" velocities, it was possible to determine the maximum swirl angle in a coordinate system moving with the disturbance. The swirl angle is defined as

$$\phi = \tan^{-1}(V(R)/Z(R))$$

where if  $U_{\text{wave}} > U_0$

$$Z(R) = U_w - U(R)$$

and if  $U_{\text{wave}} < U_0$

$$Z(R) = U(R) - U_w$$

The velocity  $U_w$  is the nondimensional wave velocity while  $V(R)$  and  $U(R)$  were defined above (and determined from curve fits of the data).

For a delta wing vortex, previous experiments show that the maximum swirl angle before breakdown is approximately  $50^\circ$ .<sup>2</sup> The maximum swirl angle for both the upstream disturbances and downstream breakdown waves is shown in fig. 17. The downstream breakdown waves had very similar values of  $\phi$ . Their values ranged from  $40^\circ$  to  $55^\circ$ . The majority of these values were near the critical angle of  $50^\circ$ .

The upstream disturbance (no breakdown) swirl angles ranged from  $55^\circ$  to nearly  $90^\circ$ . The maximum also occurs much closer to the centerline. The reason for these large values is that the axial flow in the core is very small with the defect profile. There is a lot of scatter because it was not possible to measure the upstream wave velocity accurately. Moving slightly away from the centerline the swirl velocity can become much larger than the axial velocity. Although the upstream disturbance swirl angle was greater than the critical value, no breakdown was ever observed. These data must be viewed as an atypical situation.

An important observation is that the swirl angles are all near the critical values for the breakdowns. This supports Benjamin's<sup>9</sup> established idea that vortex breakdown is a supercritical-subcritical transition.

The swirl parameter,  $q$ , was also determined with respect to the disturbance or wave velocities. The swirl parameter has been used previously to determine the stability characteristics of a columnar vortex. From previous results,<sup>23</sup> the vortex should be stable to spiral ( $n = 1$ )

disturbances if  $q > 1.58$ . Figure 18 shows a graph of the swirl parameter,  $q$ , versus the velocity defect,  $\delta$ . As shown, most of the disturbances were stable. A few actually fall in the unstable region but most are highly stable. Even though some disturbances fall in the unstable region, no significant visual difference in the disturbances was observed. Hence, we cannot attribute the turbulent disturbances to vortex instability.\*

The vortex breakdown criterion of Spall, *et. al.*<sup>29</sup> was also investigated. Figure 19 is a graph of the Rossby number versus the Reynolds number. The Rossby, a variation of the swirl angle concept, and Reynolds numbers are defined as<sup>29</sup>;

$$Ro = Z(R=1)/(r^* \Omega)$$

$$Re = r^* Z(R=1)/\nu$$

where  $Z(R=1)$  is the axial velocity at the location of maximum swirl,  $r^*$  is the location of maximum swirl,  $\nu$  is the kinematic viscosity, and  $\Omega$  is the limit of  $V/r$  as  $r$  approaches zero, i.e.

$$\Omega = \lim_{r \rightarrow 0} (V/r)$$

Spall, *et. al.* actually have two criteria levels;  $Ro < 0.6$  for wing-tip vortices and something higher, for leading edge vortices. Lacking data the leading edge value is not precisely defined.

The data for both the breakdown waves and upstream disturbances are presented. The downstream breakdowns had larger Reynolds and Rossby numbers than the upstream disturbances. The upstream disturbance data suffers from the same inaccuracies as noted with regard to Fig 17. It is not too surprising the data show no vortex breakdowns within the region where there should have been breakdowns. On the other hand the criteria was too low for the downstream breakdown waves. It should be noted that the Spall *et al.*<sup>29</sup> have breakdown data at  $Ro = 1.1$  for the leading-edge vortices. Because of the jet-like profile the downstream wave should be compared to this value. Thus, the data is consistent with a higher leading edge criteria.

---

\* The results previously published by the authors<sup>13</sup>, have been rechecked and all of the values of  $q$  were stable. The corrected results are in Stifle<sup>14</sup>.



## SUMMARY

A trailing vortex was produced which convected downstream without undergoing breakdown. Disturbances were introduced onto the vortex using a moving wire to cut the vortex. The development of upstream and downstream propagating waves was observed and wave velocities measured. The following was observed:

1. The disturbance traveling downstream propagated into a flow with a jet-like axial velocity profile. The disturbance gave the appearance of a vortex breakdown during flow visualization.

2. The wave velocity of the breakdown was greater than the freestream velocity and increased with vortex strength. This is in agreement with the wave theory of vortex breakdown.

3. The disturbance traveling upstream propagated into a flow with a wake-like defect in axial velocity. The region appeared as an expanding turbulent mixing region. It did not have the characteristics of a vortex breakdown.

4. The stagnation view, adverse pressure gradient, of vortex breakdown does not adequately describe breakdown. We did not have any external pressure gradient in our tests so the disturbances should have died out. All of the breakdowns we observed persisted throughout the test section even though we did not apply an external pressure gradient.

5. Vortex breakdown is not a result of hydrodynamic instability. The vortices produced during this project were stable but vortex breakdowns were able to be created on them.

6. The authors are unaware of any experiments with vortex breakdown which have wake-type axial profiles. All reported vortex breakdowns have shown vortices with jet-type axial profiles. This is slightly inconsistent with numerical results. On one occasion vortex breakdown has been found by numerical simulation using vortices with wake-type axial profiles.<sup>16</sup> Most researchers have used uniform axial velocity profiles for their numerical simulations. More calculations are needed on this point.

7. Any criteria which hopes to predict vortex breakdown must include effects of the axial velocity profile.

This research was supported by NASA research grant NAG-2-398.

## REFERENCES

1. Bradshaw, P., "Breakdown of a Turbulent Vortex", Presented at APS 42nd Annual Meeting of Division of Fluid Dynamics, 1989.
2. Escudier, M., "Vortex Breakdown: Observations and Explanations", *Progress in Aero. Sciences*, Vol 25, 1988, pp. 189-229.
3. Leibovich, S., "Vortex Stability and Breakdown", *AIAA Journal*, Vol. 22, Sep. 1984 , pp. 1192-1206.
4. Stuart, J. T., "A Critical Review of Vortex-Breakdown Theory", Colloquium on "Vortex Control and Breakdown Behaviour", Baden, Switzerland, April 1987
5. Hall, M. G., "Vortex Breakdown", *Annual Review of Fluid Mechanics*, Vol. 4, 1972, pp. 195-218.
6. Sarpkaya, T., "Vortex Breakdown in Swirling Conical Flows", *AIAA Journal*, Vol. 9, Sep. 1971, pp. 1792-1799.
7. Garg, A. K. and Leibovich, S., "Spectral Characteristics of Vortex Breakdown Flowfields", *Physics of Fluids*, Vol. 22, 1979, pp. 2053-2064.
8. Escudier, M. P., Bornstein, J., and Maxworthy, T., "The Dynamics of Confined Vortices", *Proceedings of the Royal Society, Series A*, 382, 1982, pp. 335-360.
9. Benjamin, T. B. , "Theory of the Vortex Breakdown Phenomenon", *Journal of Fluid Mechanics*, Vol. 14, 1962, pp. 593-629.

10. Spall, R., and Gatski, T., "A Computational Study of the Taxonomy of Vortex Breakdown", AIAA paper 90-1624, June 1990.
11. Maxworthy, T., Hopfinger, E. J., and Redekopp, L. G., "Wave motions on vortex cores", *Journal of Fluid Mechanics*, Vol. 151, 1985, pp. 141-165.
12. Reynolds, G. A. and Abtahi, A. A., "Three-Dimensional Vortex Development, Breakdown, and Control", AIAA paper 89-0998, 1989.
13. Stifle, K. E., and Panton, R. L., "Experiments concerning the Theories of Vortex Breakdown", AIAA paper 91-0736, Jan. 1991.
14. Stifle, K. E., "The Effect of Large Perturbations on a Trailing Vortex", M.S. Thesis, University of Texas at Austin, 1991.
15. Bossel, H. H., "Vortex Breakdown Flowfield", *Physics of Fluids*, Vol. 12, 1969, pp. 498-508.
16. Grabowski, W. J., and Berger, S. A., "Solutions of the Navier-Stokes Equations for Vortex Breakdown.", *Journal of Fluid Mechanics*, Vol. 75, 1976, pp. 525-544.
17. Spall, R. E., Gatski, T. B., and Ash, R. L., (1990) "The Structure and Dynamics of Bubble-Type Vortex Breakdown", *Proceedings of the Royal Society, Series A*, Vol. 429, 1990, pp. 613-637.
18. Leibovich, S., "The Structure of Vortex Breakdown" *Annual Review of Fluid Mechanics*, Vol. 10, 1978, pp. 221-246.
19. Daigle, K. J., "Vortex Response to Perturbations and to Strain Fields", M.S. Thesis, University of Texas at Austin, 1989.
20. Lambourne, N. C., and Bryer, D. W., "The Bursting of Leading-Edge Vortices: Some Observations and Discussion of the Phenomenon", Aeronautical Research Council R&M 3282, 1961.

21. Singh, P. I., and Uberoi, M. S., "Experiments on Vortex Stability", *Physic of Fluids*, Vol. 19, Dec. 1976, pp. 1858-1863.
22. Staufenbiel, R., Helming, Th., and Vitting, Th., (1987) "Controlled breakdown of Tip Vortices", Colloquium on "*Vortex Control and Breakdown Behaviour*", Baden, Switzerland, April 1987.
23. Lessen, M., Singh, P. J., and Paillet, F., "The Stability of a Trailing Line Vortex", *Journal of Fluid Mechanics*, Vol. 63, 1974, pp. 753-763.
24. Granger, R. A., "Speed of a Surge in a Bathtub Vortex", *Journal of Fluid Mechanics*, 34, 1968, pp. 651-656.
25. Lowson, M. V., "Some Experiments with Vortex Breakdown", *Journal of the Royal Aeronautical Society*, 68, 1964, pp. 343-346.
26. Falar, J. H., and Leibovich, S., "Disrupted States of Vortex Flow and Vortex Breakdown", *Physics of Fluids*, 20, 1977, pp. 1385-1400.
27. Escudier, M. P., Bornstein, J., and Zehnder, N., "Observations and LDA Measurements of Confined Vortex Flow", *Journal of Fluid Mechanics*, 98, 1980, pp. 49-63.
28. Escudier, M. P., and Zehnder, N., "Vortex-flow Regimes", *Journal of Fluid Mechanics*, 115, 1982, pp. 105-121.
29. Spall, R. E., Gatski, T. B., Grosch, C. E., "A Criterion for Vortex Breakdown", *Physics of Fluids*, Vol 30, 1987, pp.3434-3440.

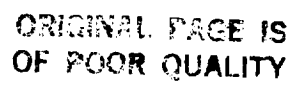
**Table 4.1: Absolute Disturbance Velocities**

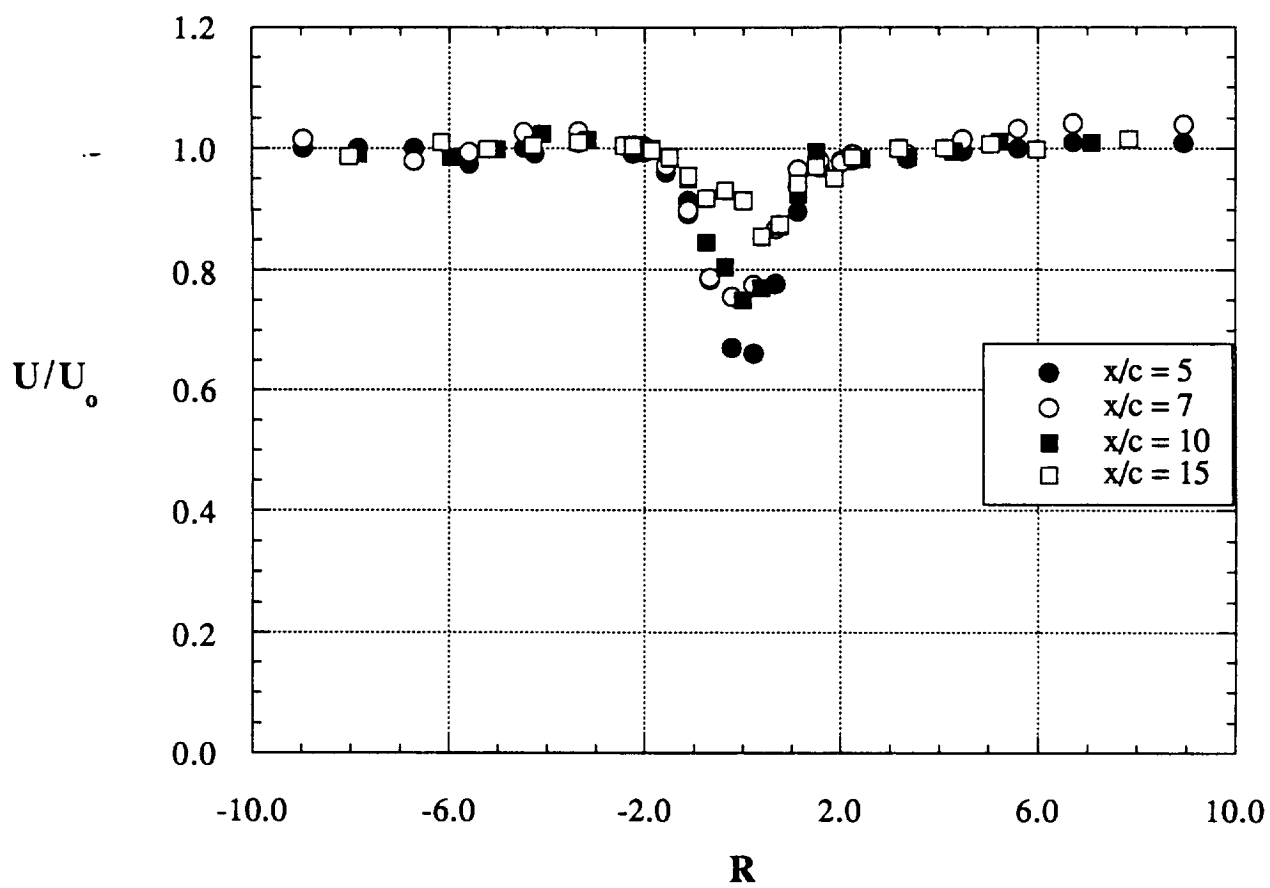
Probe (cm)	$\alpha$	$U_o$ (cm/s)	$U_{wave}/U_o$ dwn	$U_{wave}/U_o$ up
0.3175	9.4	11.62	1.25	.781
0.107	9.4	11.62	1.24	.778
0.3175	12.19	11.62	1.28	.701
0.107	12.19	11.62	1.28	.741
0.3175	9.4	17.0	1.28	.723
0.107	9.4	17.0	1.27	.710
0.3175	12.19	17.0	1.33	.598
0.107	12.19	17.0	1.32	.633
0.3175	9.4	22.6	1.29	.685
0.107	9.4	22.6	1.29	.691
0.3175	12.19	22.6	1.37	.595
0.107	12.19	22.6	1.33	.666
0.3175	9.4	25.72	1.30	.702
0.107	9.4	25.72	1.30	.702
0.3175	12.19	25.72	1.38	.572
0.107	12.19	25.72	1.35	.748

## Figure Captions

- Fig. 1 Channel set-up.
- Fig. 2 Variation of axial velocity with increasing downstream distance.
- Fig. 3 Variation of tangential velocity with increasing downstream distance.
- Fig. 4 Comparison of axial velocity measurements with curve fit.
- Fig. 5 Comparison of tangential velocity measurements with curve fit.
- Fig. 6 Schematic of absolute and relative axial velocities.
- Fig. 7 Schematic of disturbances.
- Fig. 8 Typical downstream disturbance (flow and propagation from right to left).
- Fig. 9 Typical downstream disturbance (flow and propagation from right to left).
- Fig. 10 Typical upstream disturbance (flow and propagation from right to left).
- Fig. 11 Typical upstream disturbance (flow and propagation from right to left).
- Fig. 12 Typical space-time graph of raw disturbance data; 0.3175 cm probe,  $U_0 = 22.6$  cm/s,  $\alpha = 9.4^\circ$ .
- Fig. 13 Typical space-time graph of ensemble averaged disturbance data; 0.3175 cm probe,  $U_0 = 22.6$  cm/s,  $\alpha = 9.4^\circ$ .
- Fig. 14 Variation of wave velocity with angle of attack.
- Fig. 15 Variation of wave velocity with freestream velocity.
- Fig. 16 Variation of wave velocity with probe size.
- Fig. 17 Graph of maximum swirl angle (critical angle is  $50^\circ$ )
- Fig. 18 Swirl parameter,  $q$  (Values larger than 1.58 needed for stability).
- Fig. 19 Comparison of data with vortex breakdown criteria of Spall, *et. al.*<sup>29</sup>

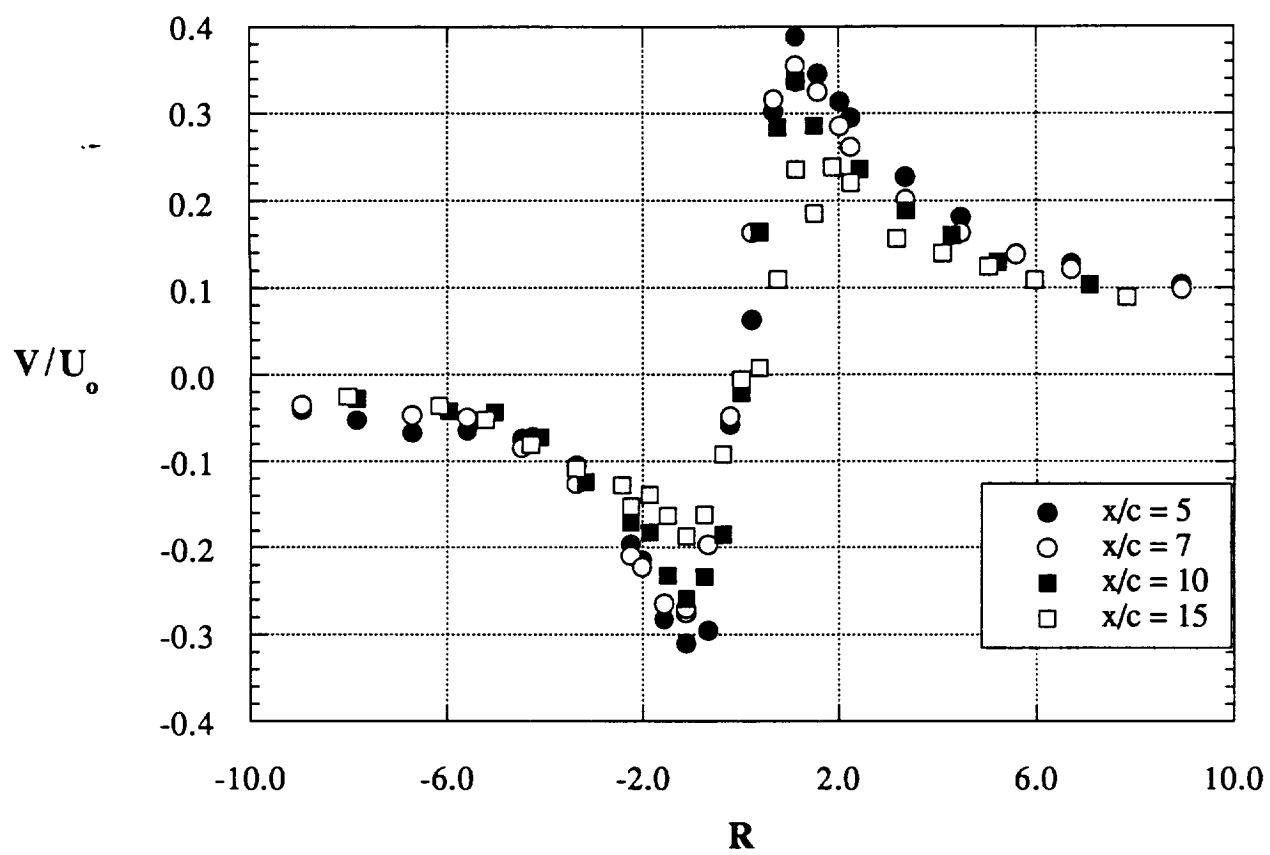
15



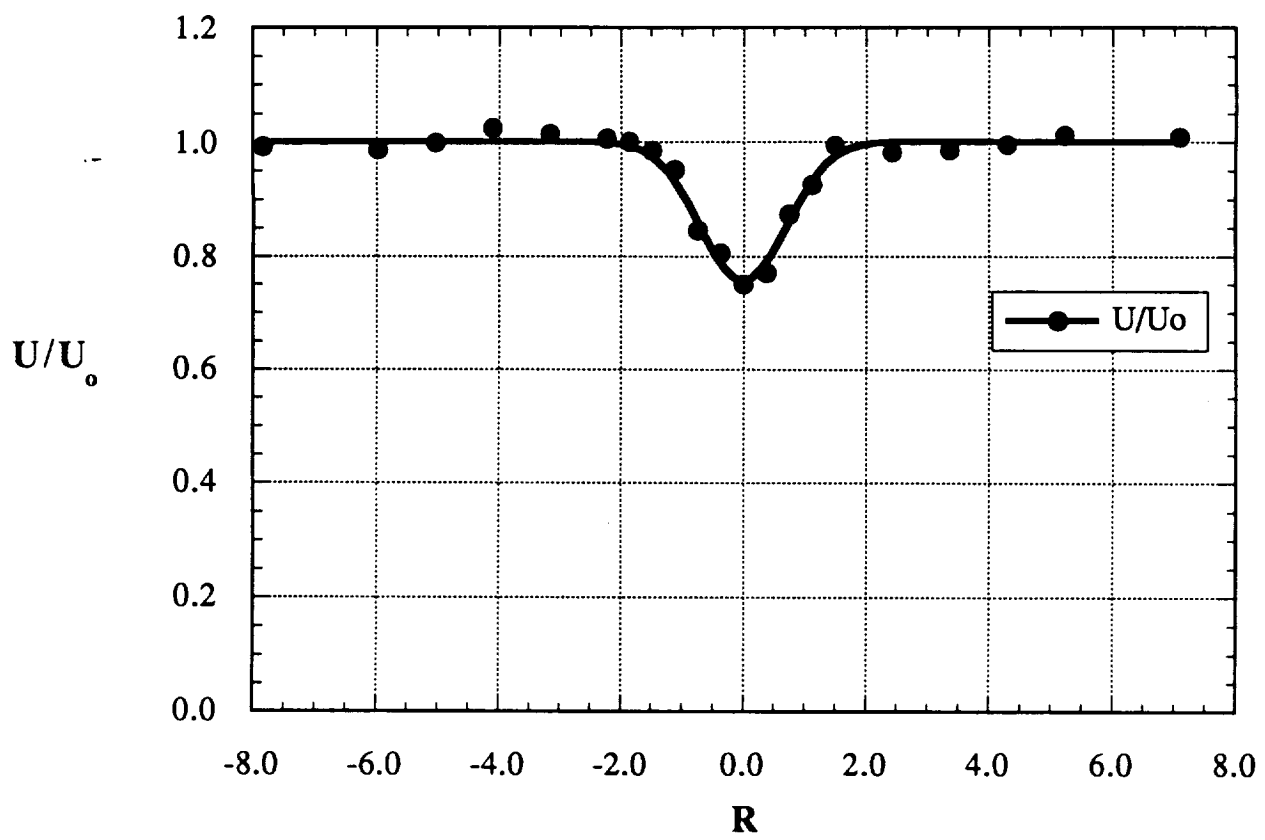


*55-116 / Panten*  
*Fig. 2*

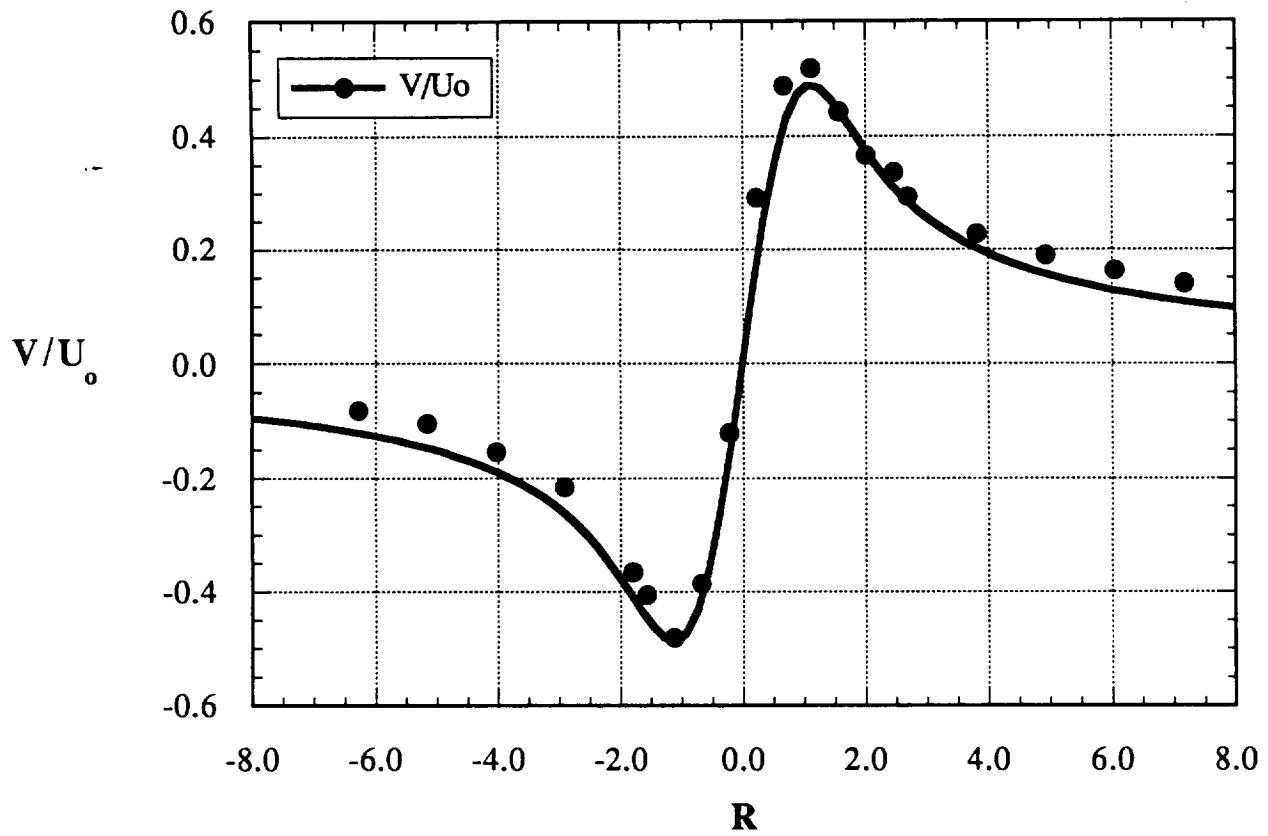




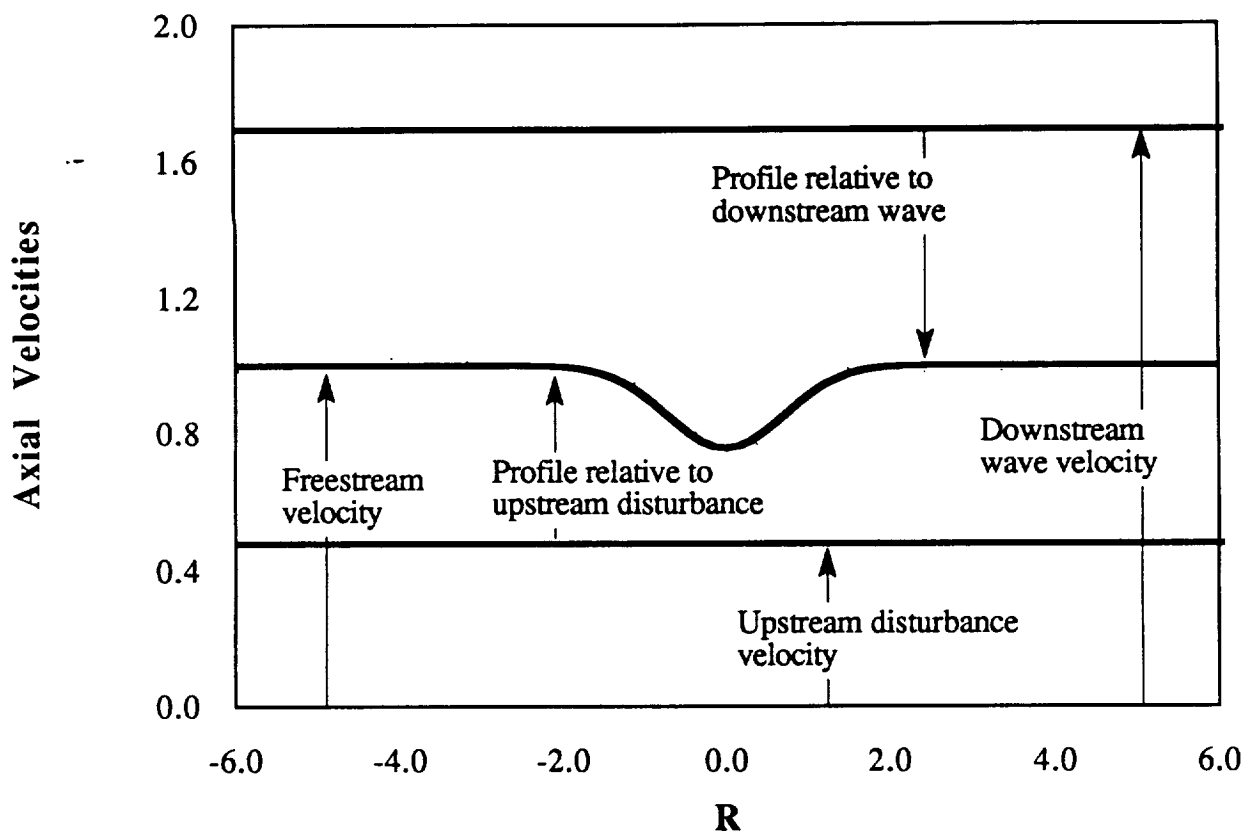
STEFLEI PANTON  
Fig. 3



STAPLE / PANTON  
Fig. 41

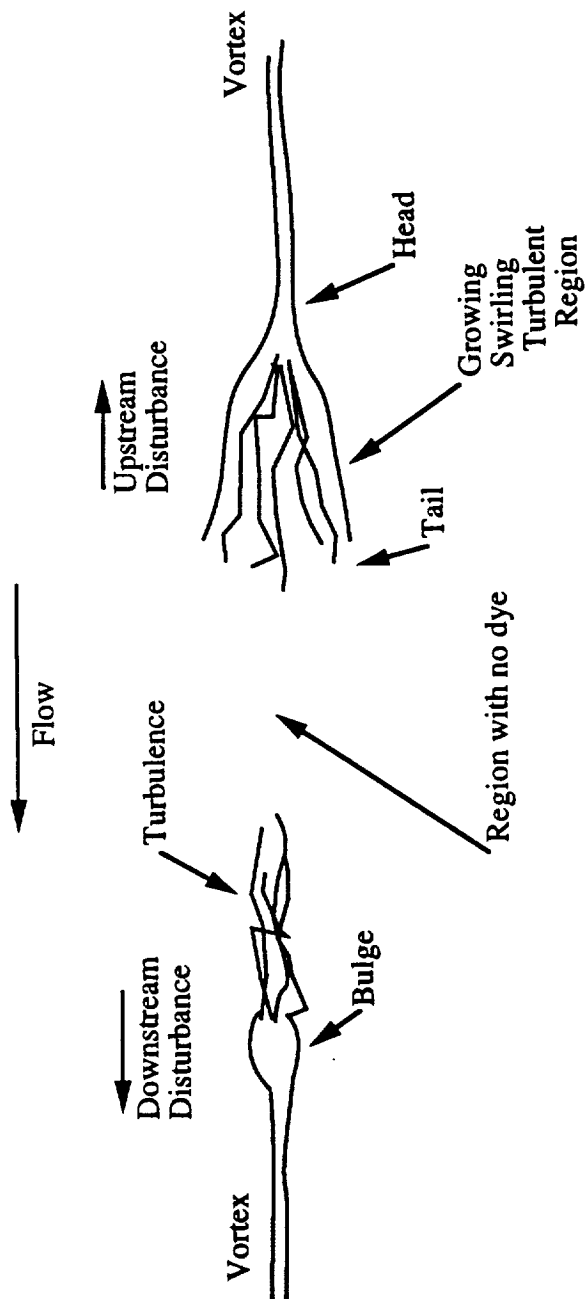


STIFLER, RANDON  
FIG. 5



STIFLE/PANTON

FIG. 6



STILL PAPER  
FIG 7

STILL PHOTO

Fig. 3



ORIGINAL PAGE IS  
OF POOR QUALITY

571546/240700  
1700 9



ORIGINAL PAGE IS  
OF POOR QUALITY

51-10-10-10-10-10

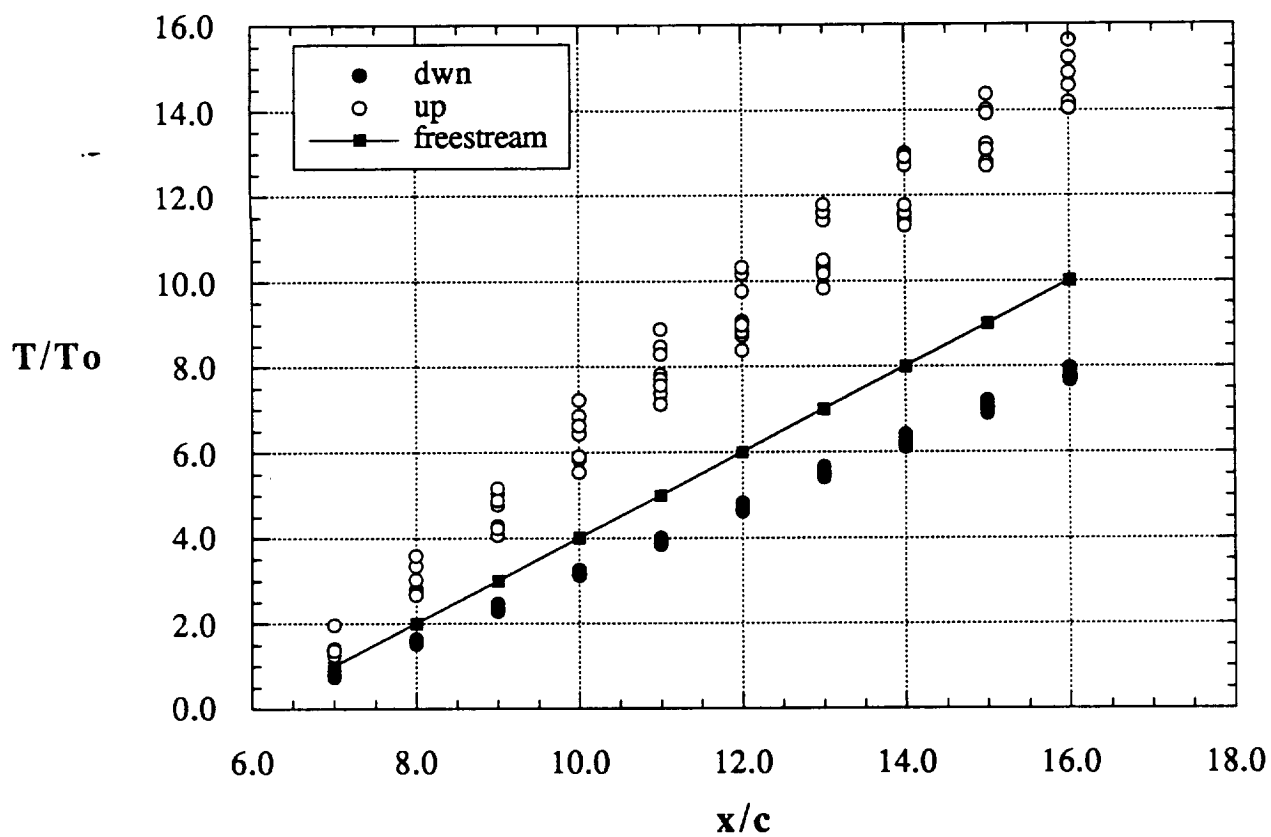
FIG. 10



ORIGINAL PAGE IS  
OF POOR QUALITY



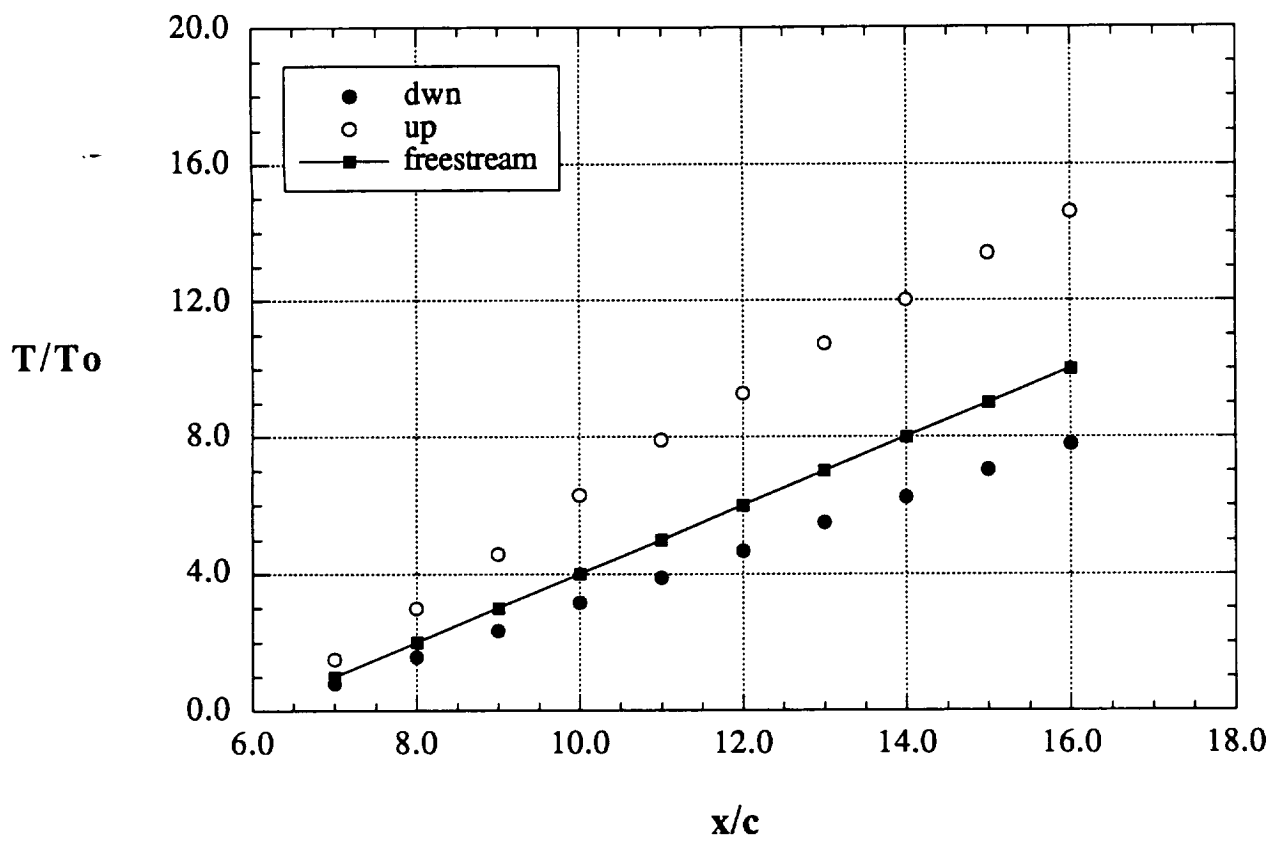




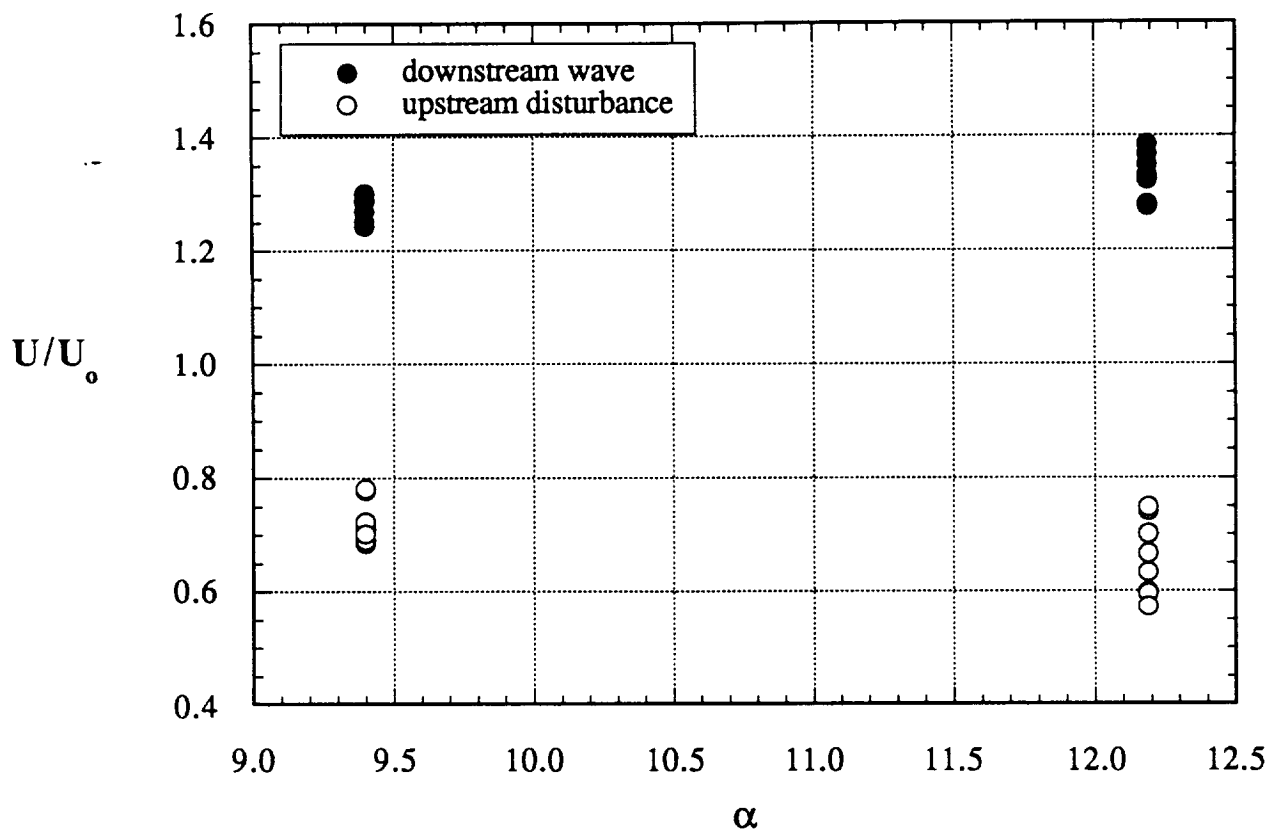
STN-10 / Pin Ton

FIG. 12

UPPER QUALITY IS  
GETTING QUALITY

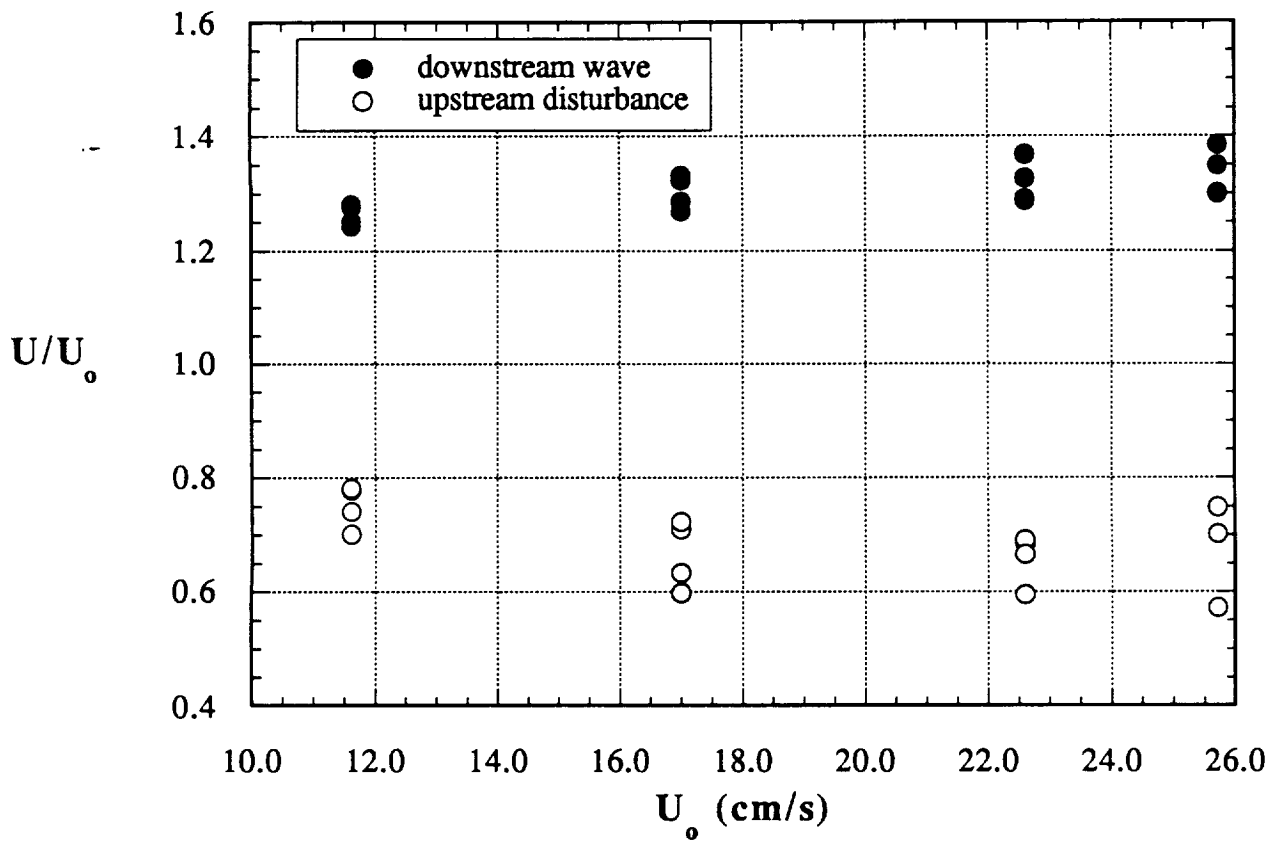


STANTON/PANTON  
FIG. 13



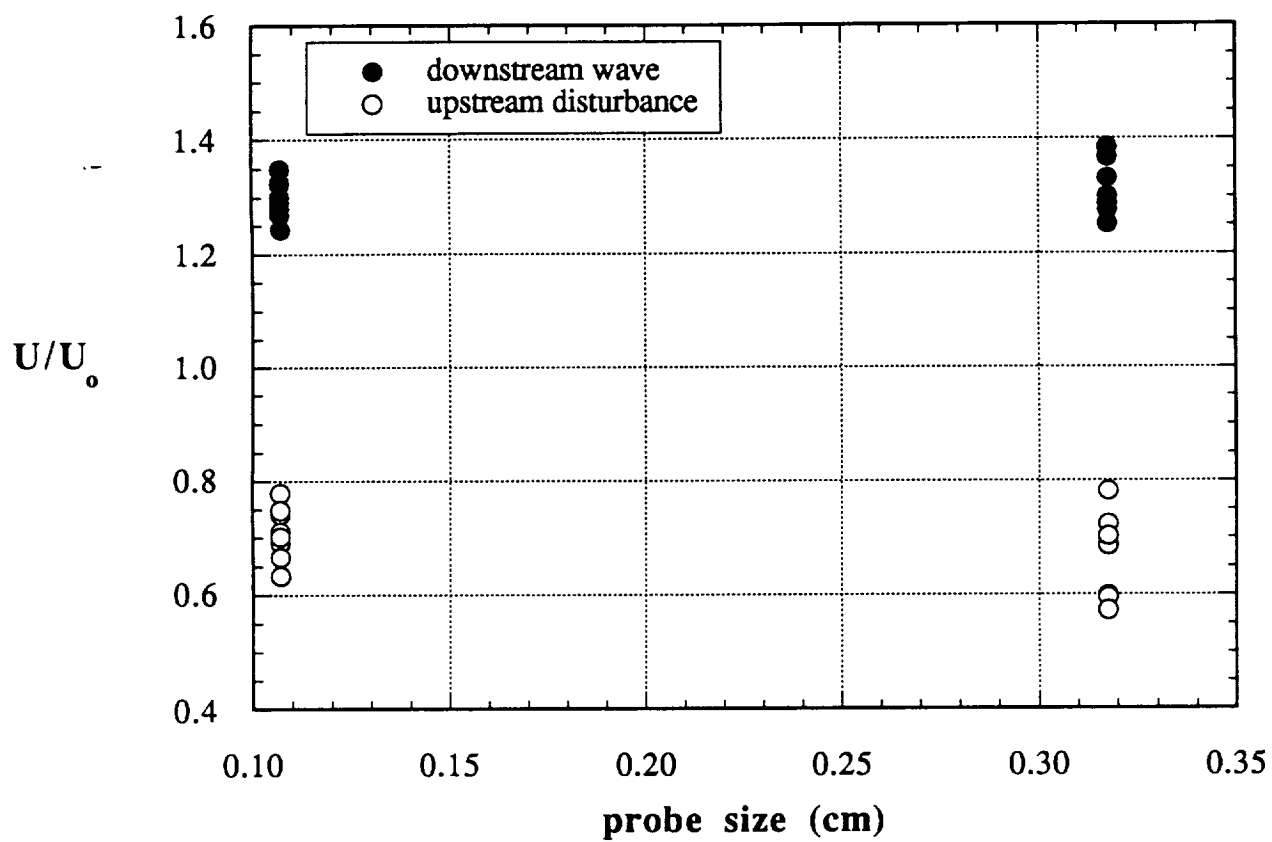
STIFLE / 179N FOR

FIG. 14



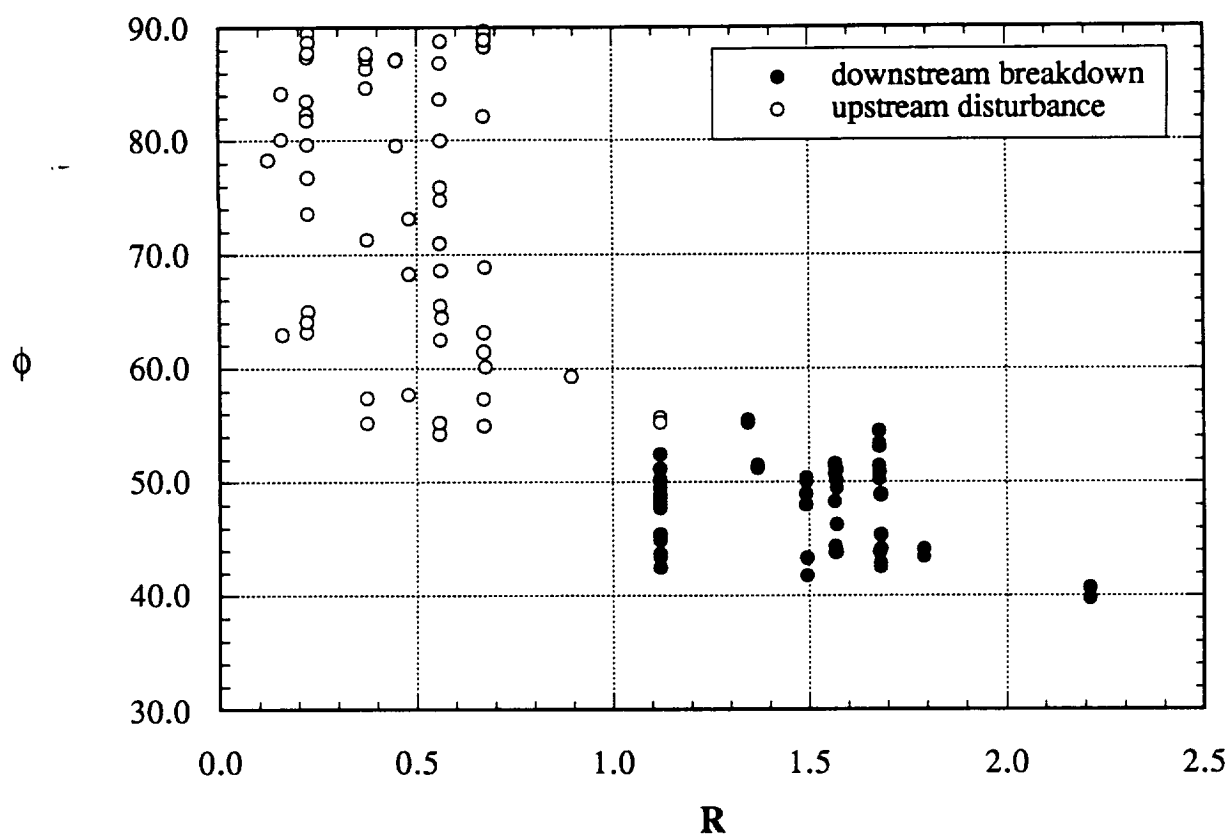
551F10/1270 T30

F13. 15



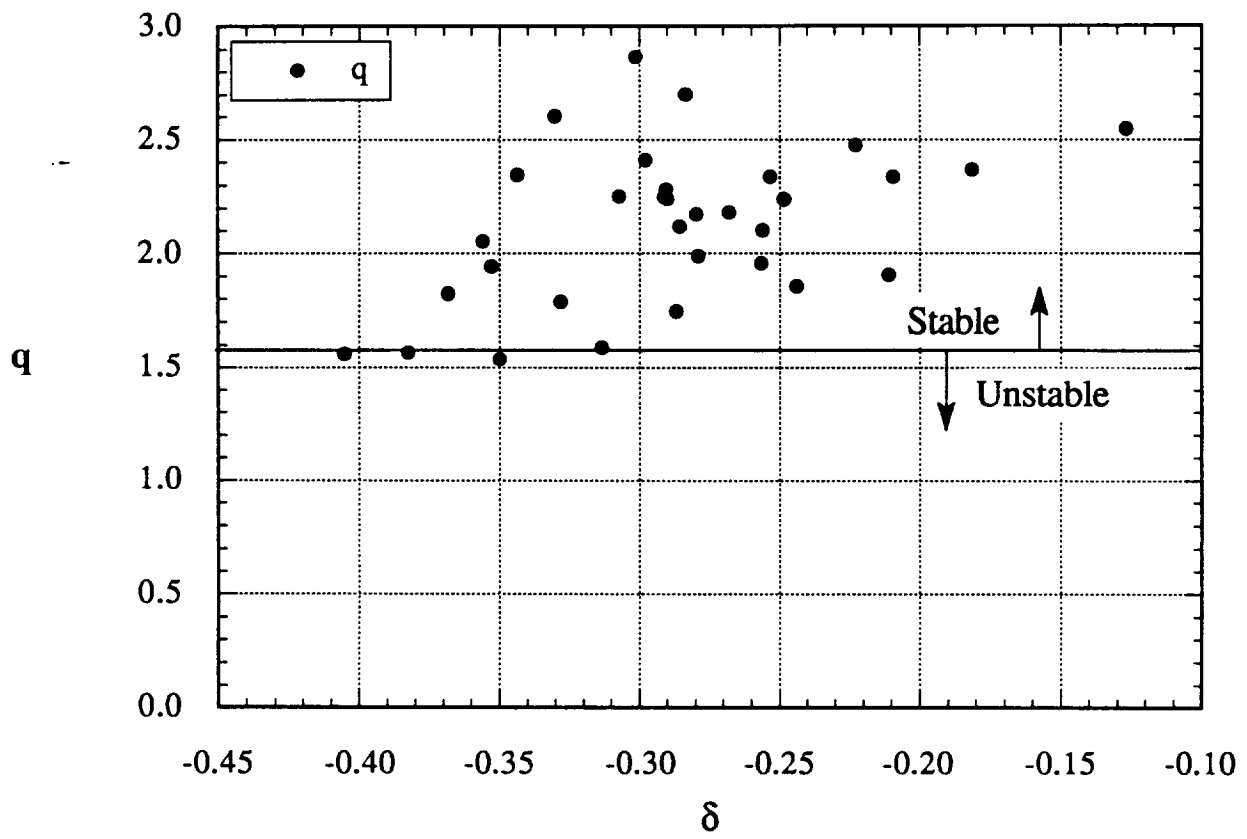
STIFEL/PANTON

FIG. 16



STEFLE / Manton

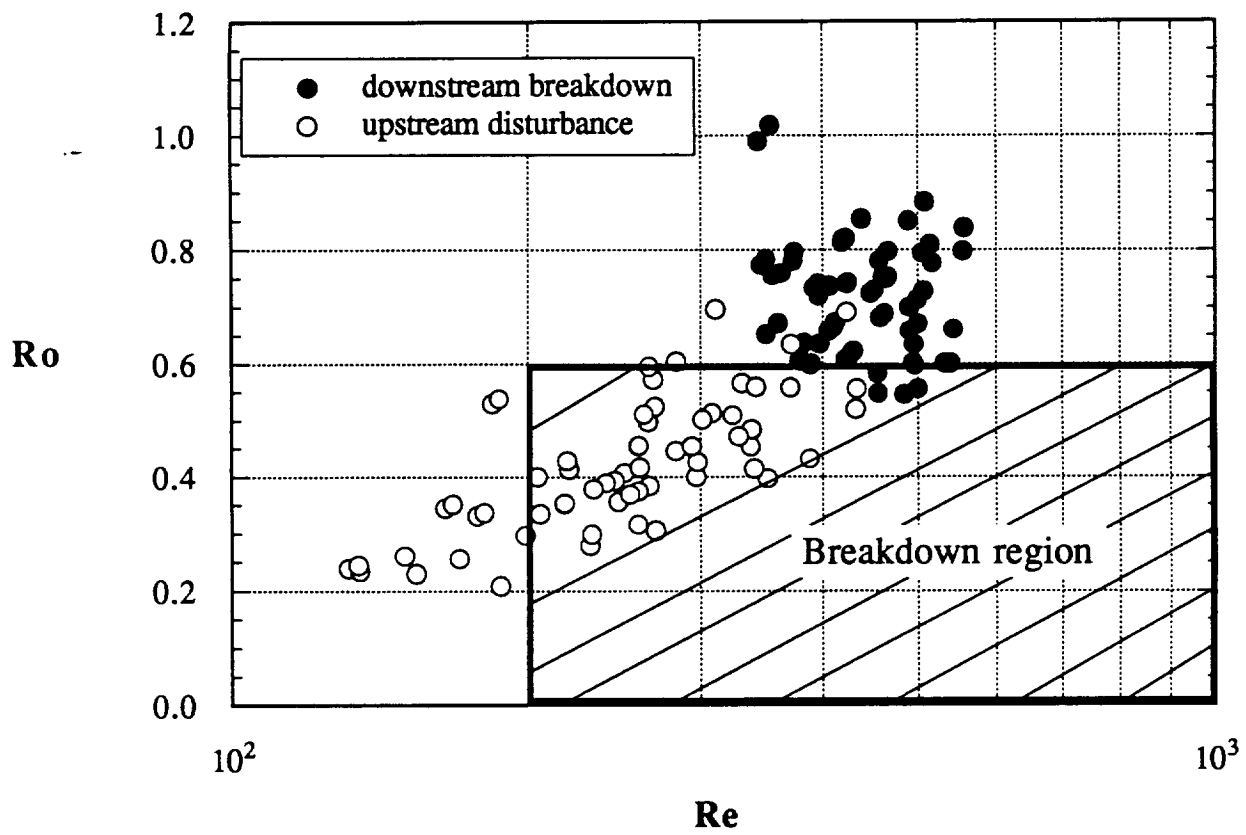
FIG. 17



STIFLE/PANTON

FIG. 15





STILL/PA-150

Fig 19